YLDL Sequence within Sendai Virus M protein is Critical for Budding of Virus-Like Particles and Interacts with Alix/AIP1 Independently of C protein

Takashi IRIE*, Yukie Shimazu, Tetsuya Yoshida, and Takemasa Sakaguchi

Department of Virology, Graduate School of Biomedical Sciences, Hiroshima University, Hiroshima 734-8551, Japan

*Corresponding author: Department of Virology, Graduate School of Biomedical Sciences, Hiroshima University, 1-2-3 Kasumi, Munami-ku, Hiroshima 734-8551, Japan

Phone: 81-82-257-5157; Fax: 81-82-257-5159; E-mail: tirie@hiroshima-u.ac.jp

Abstract

For many enveloped viruses, cellular multivesicular body (MVB) sorting machinery has been reported to be utilized for efficient viral budding. Matrix and Gag proteins have been shown to contain one or two L-domain motifs (PPxY, PT/SAP, YPDL, and FPIV), some of which interact specifically with host cellular proteins involved in multivesicular body sorting, which are recruited to the viral budding site. However, for many enveloped viruses, L-domain motifs have not yet been identified, and the involvement of MVB sorting machinery in viral budding is still unknown. Here we show that both Sendai virus (SeV) matrix protein M and accessory protein C contribute to virus budding by physically interacting with Alix/AIP1. A YLDL sequence within the M protein showed L-domain activity, and its specific interaction with the N-terminus of Alix/AIP1 (1-211) was important for the budding of virus-like particles (VLPs) of M protein. In addition, M-VLP budding was inhibited by the overexpression of some deletion mutants of Alix/AIP1 and depletion of endogenous Alix/AIP1 using specific siRNAs. The YLDL sequence was not replaceable by other L-domain motifs, such as PPxY and PT/SAP, and even YPxL. C protein was also able to physically interact with the N-terminus of Alix/AIP1 (212-357) and enhanced M-VLP budding independently of M-Alix/AIP1 interaction, although it was not released from the transfected cells itself. Our results suggest that the interaction of multiple viral proteins with Alix/AIP1 may enhance the efficiency of the utilization of cellular MVB sorting machinery for efficient SeV budding.

Introduction

Enveloped viruses bud from cellular membranes to acquire lipid-containing envelopes, and require a membrane fission event to release virions from host cells at the final step of their lifecycle. Viral matrix proteins such as Gag for retroviruses, VP40 for filoviruses, and M for rhabdoviruses have been shown to be able to bud from the cell surface by themselves in the form of lipid-enveloped, virus-like particles (VLPs), suggesting that these proteins play important roles in the late-budding step (23, 25, 28, 40, 49). Subsequent investigations have shown that these proteins possess late-budding (L) domains, which are critical for efficient budding. To date, three consensus sequences of L-domains have been identified within these matrix proteins (5). The majority of retroviruses possess PPxY- and/or PT/SAP-type L-domain motifs except for equine infectious anemia virus (EIAV), which possesses a YPxL-type L-domain motif (11). Rhabdoviruses such as vesicular stomatitis virus (VSV) and rabies virus (RV) possess a PPPY motif within M proteins, and Ebola virus possesses overlapping L-domain motifs (7-PTAP-10 and 10-PPEY-13) within VP40 (15, 22, 24, 34). More recently, another potential L-domain motif, LxxL, has been identified within HIV-1 p6 and EIAV p9, here overlapping the YPxL motif (45).

The cellular interacting partners of these L-domain motifs have also been identified. The PPxY motifs of retroviruses, rhabdoviruses, and filoviruses, and the PT/SAP motifs of HIV-1 and Ebola virus have been shown to interact with Nedd4-like E3 ubiquitin ligases via their WW domains and tumor susceptibility gene

101 (Tsg101), a member of ESCRT-I (endosomal sorting complex required for transport I), respectively (14, 16, 17). YPxL and LxxL motifs of EIAV p9 and HIV-1 p6 have been demonstrated to interact with AIP1/Alix, which has also been reported to be linked to ESCRT-I and -III complexes (9, 45). It has been suggested that L-domain motifs may function to recruit their interacting proteins to the sites of virion assembly to facilitate virus egress (5). ESCRT complexes play a critical role in sorting proteins into the multivesicular body (MVB) in mammalian cells (44). In this process, three ESCRT complexes, ESCRT-I, -II, and -III, act in a sequential manner (1, 2). In the final step of protein sorting, an AAA-type ATPase Vps4 interacts with ESCRT-III to catalyze the disassembly of ESCRT machinery to recycle its components (3, 4). The expression of dominant negative (DN) forms of and small interfering RNA (siRNA) specific for Tsg101 and Alix/AIP1 inhibit PT/SAP- and YPxL-type L-domain-mediated VLP and/or virus release, respectively (9, 12, 14, 45). In addition, in many cases, DN forms of Vps4 lacking the ability to bind or hydrolyze ATP were shown to inhibit the budding of VLPs and/or viruses containing any of the PPxY-, PT/SAP-, and YPxL-types of L-domains (12, 14, 32, 45). These observations suggest that viruses possessing these L-domain motifs generally utilize MVB sorting machinery for efficient budding; however, for many other enveloped viruses, L-domain motifs have not yet been identified, and the involvement of MVB sorting machinery in virus budding is still unknown. Recently, in addition to the major L-domain motifs, FPIV and YEIL sequences have been identified as potential L-domain motifs within paramyxovirus SV5 M, and prototype foamy virus (PFV)

Gag proteins, respectively (36, 41). However, the interacting partners of these motifs have not been identified yet (36, 41). In addition, it should be noted that SV5 M protein alone does not have the ability to bud as do VLPs and require other viral proteins for efficient budding (42).

As for Sendai virus (SeV), a prototype of the family *Paramyxoviridae*, we previously reported that C protein, one of the accessory proteins of SeV, physically interacted with Alix/AIP1, and enhanced VLP budding, possibly depending on the MVB sorting pathway, although C protein did not have the ability to form VLPs (38). Similar to SV5, other viral proteins, such as the nucleoprotein N and two glycoproteins F and HN are required for the integrity of SeV VLP formation; however, matrix (M) protein itself has the ability to be efficiently released from the cell surface in the form of VLPs, implying that M protein provides the major driving force for SeV budding, although no known L-domain motifs have been found within M protein, and any links with M protein and host factors are also not known (38, 39, 46, 47).

In this report, we intended to identify an amino acid motif within SeV M protein responsible for efficient M-VLP budding, and to investigate cellular factors involved in this function.

Materials and Methods

Cells and antibodies. Human 293T cells were maintained in Dulbecco's minimum essential medium (DMEM; Sigma) supplemented with 10% fetal bovine serum (FBS; Biological Industries, Kibbutz Beit Haemek, Israel) and penicillin-streptomycin at 37 C. Polyclonal antibodies (pAb) against the whole virion and the C protein of SeV were described previously (46). pAb against GAL4 DNA-BD (Sigma) and monoclonal antibody (mAb) against HA-tag (2C16; MBL, Nagoya, Japan) were used according to the protocols of the suppliers.

Plasmid construction. Plasmids encoding SeV M-WT, C-WT, N-WT, HN-WT, and F-WT in pCAGGS.MCS vector have been described previously (46). M gene mutants (M-A2, M-A4, M-PY, M-PY>A4, M-PT, M-PT>A4, and M-YP) were generated using a standard PCR technique, and inserted into the pCAGGS.MCS vector. A plasmid encoding 5' HA-tagged AIP1-WT in the pCAGGS.MCS vector has been described previously (38). A series of 5' HA-tagged AIP1 mutants (1-211, 1-423, 1-628, 358-868, 424-628, and 629-868) was generated using a standard PCR technique, and inserted into the pCAGGS.MCS vector. WT and/or mutant genes of M, C, and HA-tagged AIP1 were amplified by PCR, and subcloned into pM GAL4 DNA-BD and pVP16 AD cloning vectors (BD Biosciences Clontech) for mammalian two-hybrid assay. All of these constructs were confirmed by DNA sequencing.

VLP budding assay. Human 293T cells cultured in 6-well plates were transfected with the indicated plasmids using FuGENE 6 transfection reagent (Roche Diagnostics). At 24 or 48 hr post-transfection (p.t.), culture medium was harvested

and clarified at 3,000 rpm for 10 min. The supernatant was then centrifuged at 40,000 rpm for 2 hr through a 20% sucrose cushion. The pellet was suspended in 100 μl of SDS-PAGE sample buffer (125 mM Tris-HCl [pH 6.8], 4.6% sodium dodecyl sulfate [SDS], 10% dithiothreitol [DTT], 0.005% bromophenol blue, 20% glycerol), and analyzed by SDS-PAGE (10%) followed by Western blotting using anti-SeV antibody. Cell lysates were also prepared and analyzed by Western blotting using appropriate antibodies. Bands of M proteins were quantitated by densitometry with the ImageJ 1.2.4 program. VLP budding rates were calculated as the ratio of M protein in VLPs to that in cell lysates. For the experiment of Fig. 5, at 24 hr p.t., cells were metabolically labeled with 3.7 MBq/ml of [^{35}S]Met-Cys (Pro-mix; Amersham Biosciences) for 24 hr. Culture medium was harvested and clarified at 3,000 rpm for 10 min. The supernatant was then centrifuged at 40,000 rpm for 2 hr through a 20% sucrose cushion. The pellet was suspended in radioimmunoprecipitation assay (RIPA) buffer (1% Triton X-100, 1% sodium deoxycholate, 0.1% SDS, 10 mM Tris-HCl [pH 7.4], 150 mM NaCl), immunoprecipitated with anti-SeV pAb, and analyzed by SDS-PAGE. In order to examine the protein expression from transfected plasmids, cell lysates were also immunoprecipitated with the appropriate antibodies, and analyzed by SDS-PAGE. Protein bands were visualized and analyzed with a BAS2000 Bio-imaging analyzer (Fuji Film).

Pulse-chase experiment. 293T cells cultured in 6-well plates were transfected with the indicated plasmids using FuGENE 6 reagent. At 16 hr p.t., cells were

washed with PBS(-) three times, and incubated with Met-Cys-free medium (Invitrogen) for 30 min. Cells were then metabolically labeled with 3.7 MBq/ml of [^{35}S]Met-Cys for 10 min. Radioactive medium was removed, cells were washed with PBS(-), and incubated in fresh growth medium at 37 C. At the indicated time points, cells were suspended in RIPA buffer, and immunoprecipitated with anti-SeV pAb, and analyzed by SDS-PAGE. Protein bands were visualized with a BAS2000 Bio-imaging analyzer.

IP-Western. 293T cells cultured in 6-well plates were co-transfected with the indicated plasmids using FuGENE 6 reagent. At 24 hr p.t., cells were suspended in cell lysis buffer (0.5% NP-40, 20 mM Tris-HCl [pH 7.4], 150 mM NaCl) containing a "complete" protease inhibitor cocktail (Roche Diagnostics). Cell lysate samples were immunoprecipitated with either anti-SeV or -HA antibody. The immunoprecipitates by anti-SeV and -HA antibodies were separated by SDS-PAGE followed by Western blotting using anti-HA and -SeV antibodies, respectively. Protein bands were quantitated as described above. Cell lysates were also subjected directly to Western blotting using anti-HA or -SeV antibody to confirm the expression of Alix/AIP1 and M proteins, respectively.

Mammalian two-hybrid assay. BD Matchmaker Mammalian Assay Kit 2 (BD Biosciences Clontech) was used for this assay, and experiments were performed according to the protocol of the supplier. GAL4 DNA-BD and VP16 AD plasmids for this assay were prepared as described above. 293T cells were transfected with the indicated AD and BD plasmids together with a pG5SEAP reporter plasmid. At

48 hr p.t., culture medium was harvested and clarified by high-speed centrifugation. Medium samples were applied to fluorescent SEAP assay using BD Great EscAPe SEAP (BD Biosciences Clontech) to quantitate the secreted alkaline phosphatase (SEAP) activity of each sample according to the protocol of the supplier. The fluorescence of each sample was measured using a plate fluorometer (ARVO-SX; Wallac Berthold Japan, Tokyo, Japan).

siRNA transfection. Synthetic oligonucleotides were inserted between the human U6 promoter and terminator sequence of the pBAsi-hU6 vector (Takara) to generate a stem-loop type of small interfering RNA in transfected cells. pBAsi-AIP1#2147, which targeted nucleotides 2147-CCTAGTGCTCCTTCAATTC-2165 of the AIP1 gene, was constructed. A siRNA plasmid for the negative control (pBAsi-NC) was described previously (38). 293T cells in 60-mm dishes were transfected with 1 μg of the designated pBAsi plasmids. At 24 hr p.t., cells were transfected a second time with 1 μg of pCAGGS-M-WT together with 1 μg of the pBAsi plasmids. After another 24 hr, cells were metabolically labeled with [^{35}S]Met-Cys for 24 hr, and then analyzed as described above.

Results

YLDL sequence within SeV M protein is crucial for VLP budding.

In order to find an amino acid motif within SeV M protein responsible for VLP formation, we inspected the amino acid sequences of M proteins of paramyxoviruses, such as SeV, human parainfluenza virus type-1 and -3 (HPIV-1 and -3), rinderpest virus (RPV), measles virus (MeV), mumps virus (MuV), phocine distemper virus (PDV), and SV5. Three major L-domain consensus sequences, PS/TAP, PPxY, and YPxL, were not found within any of these M proteins. However, a YxxL motif closely matching the YPxL motif was found in the N-terminus of M proteins of SeV of the genus *Respiroviruses*, and RPV, PDV, and MeV of the genus *Morbilliviruses*, but not in the M proteins of MuV and SV5 of the genus *Rubulaviruses*. SeV M protein contains a YLDL sequence starting at amino acid 49, and a trace of this sequence (YLD) starting at amino acids 49 and 53 was found in the M proteins of HPIV-1 and -3 of the genus *Respiroviruses*, respectively.

To elucidate the potential function of the YLDL sequence within SeV M protein in VLP budding, we generated two mutants, M-A2 and -A4, in which Y-49 and L-52, and the entire YLDL amino acids were replaced by alanines (Fig. 1A). The ability of M-WT, -A2, and -A4 to bud as VLPs was examined using a functional budding assay (Fig. 1). 293T cells were transfected with M-WT, M-A2, and M-A4 plasmids. A striking difference in budding efficiency was observed between M-WT and M mutants (Fig. 1B). M-WT was readily detectable even at 24 hr p.t., and the amount of M-WT released in the culture medium increased with time (Fig. 1B, lanes 2 and 6).

In contrast, the release of M protein into the culture medium was dramatically reduced by amino acid changes within the YLDL sequence, although the amounts of M proteins in cell lysates were not largely different (Fig. 1B, lanes 2 to 4, and 6 to 8). Average quantitation data revealed that the budding efficiencies of M-A2 and M-A4 VLPs were approximately 30- and 200-fold reduced compared to that of M-WT, respectively (Fig. 1C). In the pulse-chase experiment, during the chase period up to 4 hr, stability of M-A4 was indistinguishable from that of M-WT, indicating that the reduced amount of the M mutants released from the transfected cells were not due to the difference in stability between M-WT and the M mutants (Fig. 1D).

These results indicate that the YLDL sequence within M protein is critical for SeV M-VLP budding.

The YLDL motif is not functionally replaceable with the major L-domain motifs.

It has been reported that, in most L-domain-identified viruses, L-domain motifs are functionally interchangeable (19, 20, 27, 31, 35, 52). We next sought to determine whether the YLDL sequence within M protein would be functionally replaceable with other types of L-domain motifs. For this purpose, chimeric M proteins (M-PY, and M-PT) were constructed, in which the YLDL motif containing the twelve amino acid region of SeV M protein were replaced by the PPPY motif-containing region from VSV and the PTAP motif-containing region from HIV-1, respectively (Fig. 2A). We also generated two more constructs (M-PY>A4 and M-PT>A4) in which the core L-domain motifs of M-PY and -PT were replaced

with four alanines, respectively (Fig. 2A). In addition, we generated an M-YP mutant, in which L-50 was replaced by a proline to possess the YPDL motif from EIAV p9 (Fig. 2A). The ability of these proteins to bud as VLPs was compared to that of M-WT using a functional budding assay as described above. Unexpectedly, unlike many other viruses containing classical L-domain motifs, the release of all these M protein mutants as VLPs was dramatically diminished compared to M-WT, although similar amounts of M protein expression in transfected cells was observed (Fig. 2B). Average quantitation data revealed that the budding efficiency of these chimeric M proteins was more than 100-fold lower than that of M-WT (Fig. 2C). These results indicate that the YLDL sequence of SeV M protein is not functionally replaceable by PPPY, PTAP, and even YPDL-types of L-domains from VSV, HIV-1, and EIAV, respectively.

Alix/AIP1 interacts with SeV M protein in a YLDL motif-dependent manner.

We next sought to determine whether SeV M protein would interact with Alix/AIP1 in a YLDL sequence-dependent manner, since YPxL and LxxL motifs have been shown to interact with Alix/AIP1 (45).

At first, we examined the SeV M-Alix/AIP1 interaction by IP-Western (Fig. 3A and 3B). 293T cells were transfected with either M-WT, -A2, -A4, or empty plasmid together with AIP1-WT. At 24 hr p.t., cell lysates were prepared, and immunoprecipitated with the designated antibodies. Immunoprecipitates were separated by SDS-PAGE, and analyzed by Western blotting using the designated antibodies. The amounts of AIP1-WT and M proteins in the transfected cells were

not largely different, respectively (Fig. 3A, lanes 15 to 18, 20, and 22 to 24). AIP1-WT was co-immunoprecipitated with M-WT, but the levels of AIP1-WT co-immunoprecipitated with M-A2 and -A4 were reduced by an average of 2.5- and 24-fold compared to that with M-WT (Fig. 3A, lanes 4 to 5, and Fig. 3B). Similarly, M-WT was co-immunoprecipitated with AIP1-WT, but M-A2 and -A4 were not (Fig. 3A, lanes 10 to 12).

We further examined the interaction between SeV M and Alix/AIP1 using a mammalian two-hybrid technique (Fig. 3C and 3D). 293T cells were co-transfected with M-WT, -A2, or -A4 fused with GAL4 DNA binding domain (BD), and AIP1-WT fused with the VP16 activation domain (AD) (Fig. 3C). Similarly, cells were co-transfected with AD-fused M protein mutants and BD-fused AIP1-WT (Fig. 3D). Almost equivalent amounts of AIP1-WT and M proteins were expressed in the transfected cells, respectively (Fig. 3C and 3D, lanes 3 to 6 and 10 to 12). Bar graphs of average SEAP activity showed the interaction of AIP1-WT with M-WT, but SEAP activity was reduced in M-A2 or -A4-transfected samples (Fig. 3C and 3D).

These results indicate that Alix/AIP1 physically interacts with SeV M protein in a YLDL sequence-dependent manner.

N-terminal 211 amino acids of Alix/AIP1 are important for interaction with M protein.

To investigate which region of Alix/AIP1 is required for interaction with M protein, a series of deletion mutants of Alix/AIP1 was generated (Fig. 4A). 293T

cells were co-transfected with BD-fused M-WT and a series of AD-fused Alix/AIP1 mutants together with the SEAP reporter plasmid, and SEAP activity at 48 hr p.t. was measured. Almost equivalent amounts of M-WT were expressed in transfected cells, and the expression of each Alix/AIP1 mutant was confirmed (Fig. 4B). Bar graphs of average SEAP activity showed that AIP1-WT as well as Alix/AIP1 mutants, AIP1(1-211), AIP1(1-423), and AIP1(1-628), containing N-terminal Bro-like domain, interacted with M-WT, but other mutants, AIP1(358-868), AIP1(424-628) and AIP1(628-868), which did not contain the domain, did not (Fig. 4C). This result indicates that the N-terminal region of Alix/AIP1 at positions of 1 to 211, including the Bro-like domain, is important for interaction with SeV M protein.

Alix/AIP1 functions in SeV M-VLP budding.

To investigate whether Alix/AIP1 would function in the budding of SeV M-VLPs, we first examined whether overexpression of the deletion mutants of Alix/AIP1 could affect the efficiency of M-VLP budding (Fig. 5). 293T cells were co-transfected with M-WT and a series of Alix/AIP1 mutants. At 24 hr p.t., cells were metabolically labeled with [^{35}S]Met-Cys for 24 hr. VLP samples and cell lysates were harvested, immunoprecipitated with anti-HA mAb or anti-SeV pAb, and analyzed by SDS-PAGE followed by autoradiography. Almost identical amounts of M-WT were expressed in transfected cells (Fig. 5A, lanes 9 to 16), and the expression of Alix/AIP1 mutants was confirmed (Fig. 5A, lanes 17 to 23). Quantitation of radioactivity revealed that the amount of M-WT in VLPs hardly changed in the presence of AIP1-WT as well as most Alix/AIP1 mutants, whereas

only approximately 20% and 40% by overexpression of AIP1(424-628) containing two C-C domains, and AIP1(1-211) containing the N-terminal Bro-like domain, respectively, compared to the empty vector-transfected sample (Fig. 5).

Furthermore, we examined the effect of the depletion of endogenous Alix/AIP1 by a specific siRNA, AIP1#2147, on the budding of M-VLPs (Fig. 6A). The expression of Alix/AIP1 from the transfected plasmid was efficiently inhibited in cells receiving AIP1#2147 (Fig. 6B). Identical protein profiles of total protein extracts from non-specific (NS) siRNA- and AIP1#2147-transfected cells were observed following staining with Coomassie blue (Fig. 6C). The amount of M-WT in VLPs was reduced by more than 90% in AIP1#2147-transfected cells, compared to that in NS siRNA-transfected cells (Fig. 6A, lanes 1 and 2, and bar graph), although the amounts of M-WT expressed in transfected cells were not largely different (Fig. 6A, lanes 3 and 4).

These results suggest that Alix/AIP1 is functionally involved in SeV M-VLP budding.

Alix/AIP1 interacts with SeV C and M proteins in different regions.

Since we previously reported that SeV C protein also physically interacted with Alix/AIP1 (38), we further investigated which region of Alix/AIP1 was required for interaction with C protein (Fig. 7). 293T cells were co-transfected with BD-fused C-WT and a series of AD-fused Alix/AIP1 mutants together with the SEAP reporter plasmid, and SEAP activity at 48 hr p.t. was determined. Similar amounts of C-WT were expressed in transfected cells, and the expression of each Alix/AIP1 mutant was

confirmed (Fig. 7A). The bar graph of average SEAP activity showed that, like SeV M protein, C-WT interacted with AIP1-WT as well as two N-terminal mutants AIP1(1-423) and AIP1(1-628) but, unlike M protein, not with the N-terminal mutant AIP1(1-211) as well as mutants AIP1(358-868), AIP1(424-628), and AIP1(628-868) (Fig. 7B). This result indicates that, unlike M protein, a SeV C-binding site is located between amino acid positions 212-357 of Alix/AIP1.

Enhancement of the budding of M-VLPs by C protein is independent of the presence of the YLDL sequence.

Finally, we investigated whether C protein would enhance the budding of VLPs of M-WT and M-A4 in the absence of other viral proteins (Fig. 8), because we previously reported that SeV C protein enhanced the budding efficiency of SeV M-VLPs in the presence of additional viral proteins, N, F, and HN, required for the integrity of virion formation (38). 293T cells were co-transfected with the plasmids indicated in the figure. At 48 hr p.t., VLP samples and cell lysates were prepared and analyzed by SDS-PAGE followed by Western blotting using anti-SeV and anti-C pAbs. As expected from the previous report that N protein was released into culture medium in the form of a nucleocapsid-like structure together with cellular RNAs (46), N protein was readily detectable in VLP samples from N gene-transfected cells regardless of the amount of M proteins released (Fig. 8A, lanes 3, 4, 7, and 8). The expression levels of each transfected protein in cells were not largely different (Fig. 8B). Consistent with our previous report (38), VLP budding of M-WT was more than 2-fold increased in the presence of C-WT as well as

additional viral proteins (Fig. 8A, lanes 3 and 4, and Fig. 8C). C-WT alone also enhanced VLP budding of M-WT approximately 2-fold (Fig. 8A, lanes 1 and 2, and Fig. 8C). M-A4 in VLPs was not detectable in the absence of additional N, F, and HN proteins due to its budding deficiency (Fig. 8A, lanes 5 and 6, and Fig. 8C), whereas approximately 5-fold enhancement of M-A4 in VLP by C-WT was observed in the presence of additional proteins (Fig. 8A, lanes 7 and 8, and Fig. 8C). This result indicates that SeV C protein enhances M-VLP budding independently of M-Alix/AIP1 interaction regardless of the presence or absence of additional viral proteins, N, F, and HN.

Discussion

The budding of enveloped RNA viruses has been extensively studied, particularly for retroviruses, since three major L-domain motifs, PPxY, PT/SAP, and YPxL were identified within Gag proteins. Common features among L-domains have been reported. L-domain motifs are functionally interchangeable (19, 20, 27, 31, 35, 52), and the budding of retroviruses possessing any of the three major types of L-domain motifs is inhibited by overexpression of DN forms of Vps4 (12, 14, 32, 45). In addition, cellular factors, such as Nedd4, Tsg101, and Alix/AIP1, which have been identified as interacting partners for PPxY, PT/SAP, and YPxL types of L-domain motifs, respectively, are components of ESCRT complexes and/or have shown some link to MVB sorting machinery (8, 32, 50). From these observations, most enveloped viruses are believed to commonly utilize cellular MVB sorting machinery for efficient budding.

In contrast, important functional differences of viral L-domains have also been reported. L-domains have been shown to function in a cell-type-dependent manner (13), and not all L-domains are functionally interchangeable (30, 51, 52). Unlike PPxY-type L-domain-containing retroviruses, budding of the PPxY motif containing rhabdoviruses and that of an Ebola VP40 mutant VP40-dPTA, in which only the PPEY motif was retained but the PTAP motif was abolished by deleting the first three PTA amino acids of the overlapping motifs, was not sensitive to DN forms of Vps4 (21). In addition, for many enveloped viruses, no L-domain motifs have been identified yet, and the involvement of MVB sorting machinery in their budding is

still unknown. As for paramyxoviruses, L-domain motifs have not been identified yet except for SV5, whose FPIV motif within M protein is reported to act as an L-domain (41).

In this report, we first found that the YLDL sequence located at the N-terminus of M protein was critical for SeV M-VLP budding. Mutations in this sequence dramatically reduced the efficiency of M-VLP budding (Fig. 1). It is unclear whether the reduced VLP budding is due to budding defect, impaired VLP assembly, disruption of M protein trafficking, or other defects in the VLP assembly and release pathway. Experiments to determine the mechanism of the reduced budding is currently under way. The YxxL sequence was also found within M proteins of other paramyxoviruses, such as RPV, PDV, and MeV belonging to *Morbilliviruses* at similar positions to the YLDL motif of SeV M, whereas *Rubulaviruses*, such as MuV and SV5, did not contain a YxxL motif as well as other known L-domain motifs within M proteins, implying that the budding mechanism of *Respiroviruses* and *Morbilliviruses* may be different from that of *Rubulaviruses*.

We also found that SeV M protein physically interacts with Alix/AIP1 via the YLDL sequence (Figs. 3 and 4). M-VLP budding was inhibited by the overexpression of two deletion mutants of Alix/AIP1, AIP1(1-211) and AIP1(424-628), and by the depletion of endogenous Alix/AIP1 using RNAi technique (Figs. 5 and 6), suggesting that Alix/AIP1 is functionally involved in SeV M-VLP budding. Since it contains a SeV M binding site, the AIP1(1-211) mutant may interfere with the interaction between intact Alix/AIP1 and the M proteins.

Overexpression of DN forms of the components of endosomal sorting machinery, such as Vps4, CHMP4B, and Tsg101 induces formation of aberrantly enlarged endosomes (called "class E" compartment in yeast) that are defective in the sorting and recycling of endocytosed substrates (6, 7, 18). AIP1(1-211) and/or AIP1(424-628) not containing a SeV M binding site may inhibit budding by interfering with some functions of Alix/AIP1, which are utilized for the budding process. Inconsistent with our previous report that overexpression of Alix/AIP1 accelerated SeV release from the infected cells (38), budding of M-VLP was not enhanced by Alix/AIP1 overexpression (Fig. 5). This difference seems likely due to the presence or absence of the other viral proteins. As expected, no interaction of SeV M with Tsg101 and Nedd4, which have been known to interact with PT/SAP and PPxY types of L-domain motifs, and no inhibitory effect on M-VLP budding by DN forms of Tsg101 and Nedd4 were observed (data not shown).

In contrast to SeV, the FPIV motif within SV5 M protein is reported not to interact with Alix/AIP1, although it resembles the YPxL motif that interacts with Alix/AIP1 (41). Recently, another YxxL-type motif, YEIL, has also been identified as a potential L-domain within the Gag protein of prototype foamy virus (36). The YEIL motif is also reported not to interact with Alix/AIP1, although its binding partner has not been identified yet (36). Unlike SeV, it has been reported that a single expression of SV5 M protein is not enough to form VLPs, and that multiple viral proteins are required for the formation and budding of VLPs (42). These differences between SeV and SV5 may reflect their different mechanism in budding.

In spite of the functional differences of the L-domain motif of SeV M from those of other viruses, all these viruses also seem to utilize MVB sorting machinery for efficient budding, since DN forms of Vps4 block VLP and/or virus budding of all these viruses (36, 38, 42).

In addition to SV5, the contribution of multiple viral proteins for efficient VLP budding has been reported in some enveloped viruses. It is known that VLP budding by a matrix protein is enhanced in the presence of additional viral proteins, such as VSV G, Ebola virus GP and NP, although the mechanism for such enhancement remains to be determined (29, 37, 43). We previously reported that SeV C protein enhanced SeV M-VLP budding in the presence of additional viral N, F, and HN proteins, and interaction between C and Alix/AIP1 correlated with this enhancement (38). Interestingly, we found that SeV M protein also physically interact with Alix/AIP1 at the distinct region on Alix/AIP1 from C protein (amino acid positions 1-211 for M, and 212-357 for C) (Figs. 4 and 7). The C protein does not have any known amino acid motifs responsible for interaction with Alix/AIP1. Chen *et al*. demonstrated that the EIAV YPDL motif interacted with a region of Alix/AIP1 spanning amino acids 409-715 (9). This discrepancy might reflect differences in the experimental system used, or differences in L-domain function between the SeV YLDL and the EIAV YPDL motifs. Interaction between SeV M and Alix/AIP1 seems more important for VLP budding than that between C protein and Alix/AIP1, because C protein itself does not have the ability to be released from cells, and budding of SeV M-VLP was dramatically inhibited by mutations in the

YLDL motif causing loss of M-Alix/AIP1 interaction. Our results also showed that C protein could enhance SeV M-VLP budding regardless of the presence or absence of other viral proteins and independently of M-Alix/AIP1 interaction (Fig. 8). From these results, SeV M protein is by itself able to bud from the cell surface in the form of VLPs by interacting with Alix/AIP1, whereas SeV C protein may provide more Alix/AIP1 by C-Alix/AIP1 interaction and enhance efficiency to utilize cellular MVB sorting machinery for efficient VLP and/or virus budding. It will be interest to elucidate the mechanism of how SeV M and C proteins utilize Alix/AIP1 functions and cooperate with each other for efficient budding. Recently, HIV-1 Nef has been reported to interact with Alix/AIP1, resulting in the proliferation of multivesicular bodies and enhancement of budding efficiency, in addition to the interaction of Gag with Tsg101 and Alix/AIP1 via its PTAP and LxxL motifs, respectively (10). Alix/AIP1 is not only a component of MVB sorting machinery, but also has the ability to generate an MVB-resembling membrane structure *in vitro* in the presence of a specific phospholipid, lysobisphosphatidic acid, and to form exosomes, small membrane structures that are liberated from cells (33, 48). Such functions of Alix/AIP1 itself may contribute to increase the efficiency of virus budding in addition to MVB sorting machinery.

Finally, the SeV YLDL motif is similar to the EIAV YPDL motif, in terms of their importance in VLP budding, closely matching amino acid sequences, and ability to interact with Alix/AIP1. However, important differences are also observed. The YLDL motif is unique in not containing a proline residue, different

from most other L-domain motifs. The SeV YLDL motif-binding site was mapped to a region of Alix/AIP1 (amino acid positions 1-211), whereas the EIAV YPDL motif interacted with a different region of Alix/AIP1 (amino acid positions 409-715), as mentioned above (9). Surprisingly, the YLDL motif was not functionally replaceable with even the EIAV YPDL motif as well as the VSV PPPY and HIV-1 PTAP motifs (Fig. 2). These findings might imply fundamental differences in the budding mechanisms mediated by the SeV YLDL motif and the other characterized L-domain motifs.

Acknowledgements

We would like to thank the staff of the Research Center for Molecular Medicine and the Analysis Center of Life Science, Hiroshima University for the use of their facilities. This work was supported by Grants-in-Aid for Scientific Research from the Japan Society of the Promotion of Science and the Ministry of Education, Culture, Sports, Science and Technology.

References

1. **Babst, M., D. J. Katzmann, E. J. Estepa-Sabal, T. Meerloo, and S. D. Emr.** 2002. Escrt-III: an endosome-associated heterooligomeric protein complex required for mvb sorting. Dev Cell **3:**271-82.

2. **Babst, M., D. J. Katzmann, W. B. Snyder, B. Wendland, and S. D. Emr.** 2002. Endosome-associated complex, ESCRT-II, recruits transport machinery for protein sorting at the multivesicular body. Dev Cell **3:**283-9.

3. **Babst, M., T. K. Sato, L. M. Banta, and S. D. Emr.** 1997. Endosomal transport function in yeast requires a novel AAA-type ATPase, Vps4p. Embo J **16:**1820-31.

4. **Babst, M., B. Wendland, E. J. Estepa, and S. D. Emr.** 1998. The Vps4p AAA ATPase regulates membrane association of a Vps protein complex required for normal endosome function. Embo J **17:**2982-93.

5. **Bieniasz, P. D.** 2006. Late budding domains and host proteins in enveloped virus release. Virology **344:**55-63.

6. **Bishop, N., and P. Woodman.** 2000. ATPase-defective mammalian VPS4 localizes to aberrant endosomes and impairs cholesterol trafficking. Mol Biol Cell **11:**227-39.

7. **Bishop, N., and P. Woodman.** 2001. TSG101/mammalian VPS23 and mammalian VPS28 interact directly and are recruited to VPS4-induced endosomes. J Biol Chem **276:**11735-42.

8. **Blot, V., F. Perugi, B. Gay, M. C. Prevost, L. Briant, F. Tangy, H. Abriel,**

O. Staub, M. C. Dokhelar, and C. Pique. 2004. Nedd4.1-mediated ubiquitination and subsequent recruitment of Tsg101 ensure HTLV-1 Gag trafficking towards the multivesicular body pathway prior to virus budding. J Cell Sci **117:**2357-67.

9. **Chen, C., O. Vincent, J. Jin, O. A. Weisz, and R. C. Montelaro.** 2005. Functions of early (AP-2) and late (AIP1/ALIX) endocytic proteins in equine infectious anemia virus budding. J Biol Chem **280:**40474-80.

10. **Costa, L. J., N. Chen, A. Lopes, R. S. Aguiar, A. Tanuri, A. Plemenitas, and B. M. Peterlin.** 2006. Interactions between Nef and AIP1 proliferate multivesicular bodies and facilitate egress of HIV-1. Retrovirology **3:**33.

11. **Demirov, D. G., and E. O. Freed.** 2004. Retrovirus budding. Virus Res **106:**87-102.

12. **Demirov, D. G., A. Ono, J. M. Orenstein, and E. O. Freed.** 2002. Overexpression of the N-terminal domain of TSG101 inhibits HIV-1 budding by blocking late domain function. Proc Natl Acad Sci U S A **99:**955-60.

13. **Demirov, D. G., J. M. Orenstein, and E. O. Freed.** 2002. The late domain of human immunodeficiency virus type 1 p6 promotes virus release in a cell type-dependent manner. J Virol **76:**105-17.

14. **Garrus, J. E., U. K. von Schwedler, O. W. Pornillos, S. G. Morham, K. H. Zavitz, H. E. Wang, D. A. Wettstein, K. M. Stray, M. Cote, R. L. Rich, D. G. Myszka, and W. I. Sundquist.** 2001. Tsg101 and the vacuolar protein sorting pathway are essential for HIV-1 budding. Cell **107:**55-65.

15. **Hartlieb, B., and W. Weissenhorn.** 2006. Filovirus assembly and budding. Virology **344:**64-70.

16. **Harty, R. N., M. E. Brown, G. Wang, J. Huibregtse, and F. P. Hayes.** 2000. A PPxY motif within the VP40 protein of Ebola virus interacts physically and functionally with a ubiquitin ligase: implications for filovirus budding. Proc Natl Acad Sci U S A **97:**13871-6.

17. **Harty, R. N., J. Paragas, M. Sudol, and P. Palese.** 1999. A proline-rich motif within the matrix protein of vesicular stomatitis virus and rabies virus interacts with WW domains of cellular proteins: implications for viral budding. J Virol **73:**2921-9.

18. **Howard, T. L., D. R. Stauffer, C. R. Degnin, and S. M. Hollenberg.** 2001. CHMP1 functions as a member of a newly defined family of vesicle trafficking proteins. J Cell Sci **114:**2395-404.

19. **Irie, T., J. M. Licata, and R. N. Harty.** 2005. Functional characterization of Ebola virus L-domains using VSV recombinants. Virology **336:**291-8.

20. **Irie, T., J. M. Licata, H. R. Jayakar, M. A. Whitt, P. Bell, and R. N. Harty.** 2004. Functional analysis of late-budding domain activity associated with the PSAP motif within the vesicular stomatitis virus M protein. J Virol **78:**7823-7.

21. **Irie, T., J. M. Licata, J. P. McGettigan, M. J. Schnell, and R. N. Harty.** 2004. Budding of PPxY-containing rhabdoviruses is not dependent on host proteins TGS101 and VPS4A. J Virol **78:**2657-65.

22. **Jasenosky, L. D., and Y. Kawaoka.** 2004. Filovirus budding. Virus Res **106:**181-8.

23. **Jasenosky, L. D., G. Neumann, I. Lukashevich, and Y. Kawaoka.** 2001. Ebola virus VP40-induced particle formation and association with the lipid bilayer. J Virol **75:**5205-14.

24. **Jayakar, H. R., E. Jeetendra, and M. A. Whitt.** 2004. Rhabdovirus assembly and budding. Virus Res **106:**117-32.

25. **Justice, P. A., W. Sun, Y. Li, Z. Ye, P. R. Grigera, and R. R. Wagner.** 1995. Membrane vesiculation function and exocytosis of wild-type and mutant matrix proteins of vesicular stomatitis virus. J Virol **69:**3156-60.

26. **Katoh, K., H. Shibata, H. Suzuki, A. Nara, K. Ishidoh, E. Kominami, T. Yoshimori, and M. Maki.** 2003. The ALG-2-interacting protein Alix associates with CHMP4b, a human homologue of yeast Snf7 that is involved in multivesicular body sorting. J Biol Chem **278:**39104-13.

27. **Li, F., C. Chen, B. A. Puffer, and R. C. Montelaro.** 2002. Functional replacement and positional dependence of homologous and heterologous L domains in equine infectious anemia virus replication. J Virol **76:**1569-77.

28. **Li, Y., L. Luo, M. Schubert, R. R. Wagner, and C. Y. Kang.** 1993. Viral liposomes released from insect cells infected with recombinant baculovirus expressing the matrix protein of vesicular stomatitis virus. J Virol **67:**4415-20.

29. **Licata, J. M., R. F. Johnson, Z. Han, and R. N. Harty.** 2004. Contribution

of ebola virus glycoprotein, nucleoprotein, and VP24 to budding of VP40 virus-like particles. J Virol **78:**7344-51.

30. **Martin-Serrano, J., D. Perez-Caballero, and P. D. Bieniasz.** 2004. Context-dependent effects of L domains and ubiquitination on viral budding. J Virol **78:**5554-63.

31. **Martin-Serrano, J., T. Zang, and P. D. Bieniasz.** 2001. HIV-1 and Ebola virus encode small peptide motifs that recruit Tsg101 to sites of particle assembly to facilitate egress. Nat Med **7:**1313-9.

32. **Martin-Serrano, J., T. Zang, and P. D. Bieniasz.** 2003. Role of ESCRT-I in retroviral budding. J Virol **77:**4794-804.

33. **Matsuo, H., J. Chevallier, N. Mayran, I. Le Blanc, C. Ferguson, J. Faure, N. S. Blanc, S. Matile, J. Dubochet, R. Sadoul, R. G. Parton, F. Vilbois, and J. Gruenberg.** 2004. Role of LBPA and Alix in multivesicular liposome formation and endosome organization. Science **303:**531-4.

34. **Noda, T., H. Sagara, E. Suzuki, A. Takada, H. Kida, and Y. Kawaoka.** 2002. Ebola virus VP40 drives the formation of virus-like filamentous particles along with GP. J Virol **76:**4855-65.

35. **Parent, L. J., R. P. Bennett, R. C. Craven, T. D. Nelle, N. K. Krishna, J. B. Bowzard, C. B. Wilson, B. A. Puffer, R. C. Montelaro, and J. W. Wills.** 1995. Positionally independent and exchangeable late budding functions of the Rous sarcoma virus and human immunodeficiency virus Gag proteins. J Virol **69:**5455-60.

36. **Patton, G. S., S. A. Morris, W. Chung, P. D. Bieniasz, and M. O. McClure.** 2005. Identification of domains in gag important for prototypic foamy virus egress. J Virol **79:**6392-9.

37. **Robison, C. S., and M. A. Whitt.** 2000. The membrane-proximal stem region of vesicular stomatitis virus G protein confers efficient virus assembly. J Virol **74:**2239-46.

38. **Sakaguchi, T., A. Kato, F. Sugahara, Y. Shimazu, M. Inoue, K. Kiyotani, Y. Nagai, and T. Yoshida.** 2005. AIP1/Alix is a binding partner of Sendai virus C protein and facilitates virus budding. J Virol **79:**8933-41.

39. **Sakaguchi, T., T. Uchiyama, Y. Fujii, K. Kiyotani, A. Kato, Y. Nagai, A. Kawai, and T. Yoshida.** 1999. Double-layered membrane vesicles released from mammalian cells infected with Sendai virus expressing the matrix protein of vesicular stomatitis virus. Virology **263:**230-43.

40. **Sakalian, M., and E. Hunter.** 1998. Molecular events in the assembly of retrovirus particles. Adv Exp Med Biol **440:**329-39.

41. **Schmitt, A. P., G. P. Leser, E. Morita, W. I. Sundquist, and R. A. Lamb.** 2005. Evidence for a new viral late-domain core sequence, FPIV, necessary for budding of a paramyxovirus. J Virol **79:**2988-97.

42. **Schmitt, A. P., G. P. Leser, D. L. Waning, and R. A. Lamb.** 2002. Requirements for budding of paramyxovirus simian virus 5 virus-like particles. J Virol **76:**3952-64.

43. **Schnell, M. J., L. Buonocore, E. Boritz, H. P. Ghosh, R. Chernish, and J.**

K. Rose. 1998. Requirement for a non-specific glycoprotein cytoplasmic domain sequence to drive efficient budding of vesicular stomatitis virus. Embo J **17:**1289-96.

44. **Slagsvold, T., K. Pattni, L. Malerod, and H. Stenmark.** 2006. Endosomal and non-endosomal functions of ESCRT proteins. Trends Cell Biol **16:**317-26.

45. **Strack, B., A. Calistri, S. Craig, E. Popova, and H. G. Gottlinger.** 2003. AIP1/ALIX is a binding partner for HIV-1 p6 and EIAV p9 functioning in virus budding. Cell **114:**689-99.

46. **Sugahara, F., T. Uchiyama, H. Watanabe, Y. Shimazu, M. Kuwayama, Y. Fujii, K. Kiyotani, A. Adachi, N. Kohno, T. Yoshida, and T. Sakaguchi.** 2004. Paramyxovirus Sendai virus-like particle formation by expression of multiple viral proteins and acceleration of its release by C protein. Virology **325:**1-10.

47. **Takimoto, T., K. G. Murti, T. Bousse, R. A. Scroggs, and A. Portner.** 2001. Role of matrix and fusion proteins in budding of Sendai virus. J Virol **75:**11384-91.

48. **Thery, C., M. Boussac, P. Veron, P. Ricciardi-Castagnoli, G. Raposo, J. Garin, and S. Amigorena.** 2001. Proteomic analysis of dendritic cell-derived exosomes: a secreted subcellular compartment distinct from apoptotic vesicles. J Immunol **166:**7309-18.

49. **Timmins, J., S. Scianimanico, G. Schoehn, and W. Weissenhorn.** 2001.

Vesicular release of ebola virus matrix protein VP40. Virology **283:**1-6.

50. **von Schwedler, U. K., M. Stuchell, B. Muller, D. M. Ward, H. Y. Chung, E. Morita, H. E. Wang, T. Davis, G. P. He, D. M. Cimbora, A. Scott, H. G. Krausslich, J. Kaplan, S. G. Morham, and W. I. Sundquist.** 2003. The protein network of HIV budding. Cell **114:**701-13.

51. **Xiang, Y., C. E. Cameron, J. W. Wills, and J. Leis.** 1996. Fine mapping and characterization of the Rous sarcoma virus Pr76gag late assembly domain. J Virol **70:**5695-700.

52. **Yuan, B., S. Campbell, E. Bacharach, A. Rein, and S. P. Goff.** 2000. Infectivity of Moloney murine leukemia virus defective in late assembly events is restored by late assembly domains of other retroviruses. J Virol **74:**7250-60.

Figure Legends

Fig. 1. Budding assay of SeV M proteins. (A) Schematic representation of expression plasmids encoding M-WT, -A2, and -A4. (B) M proteins were expressed in 293T cells. At the indicated time points, cell lysates and VLPs in culture medium were harvested, and analyzed by SDS-PAGE followed by Western blotting using anti-SeV pAb. (C) M proteins in VLPs and cell lysates were quantitated by densitometry with ImageJ software. The values of M protein in VLPs were normalized by those in cell lysates. The level of M-WT at each time point was set to 1, and the relative values of M-A2 and -A4 are indicated. Bars represent an average of at least three independent experiments. Error bars indicate standard deviations. (D) Pulse-chase experiments for M-WT and M-A4. 293T cells transfected with M-WT and M-A4 were pulse-labeled with [^{35}S]Met-Cys for 10 min. At the indicated time points, cell lysates were prepared, immunoprecipitated by anti-SeV pAb, and analyzed by SDS-PAGE. Protein bands were visualized with a BAS2000 Bio-imaging analyzer.

Fig. 2. Budding assay of SeV M mutants possessing the VSV PPPY and HIV-1 PTAP motif-containing regions or the EIAV YPDL motif. (A) The amino acid sequence within the YLDL motif-containing region (amino acids 45 to 56) is shown for M-WT, -PY, -PY>A4, -PT, -PT>A4, and -YP as shown in Fig. 1. (B and C) These mutants were subjected to a functional budding assay, and results are shown in Fig. 1. The bar graph represents an average of at least three independent experiments.

Fig. 3. Interaction between SeV M and Alix/AIP1. (A) IP-Western study for M mutants and Alix/AIP1. 293T cells were co-transfected with the indicated plasmids. At 24 hr p.t., cell lysates were harvested, and immunoprecipitated by the indicated Abs. The immunoprecipitates were then analyzed by Western blotting using the indicated Abs. (B) Alix/AIP1 protein immunoprecipitated with anti-SeV pAb and M proteins in cell lysates was quantitated by densitometry with ImageJ software. The level of Alix/AIP1 from the sample co-transfected with M-WT was set to 1, and the relative values of Alix/AIP1 were normalized by those of M proteins in cell lysates. Bars represent an average of three independent experiments. (C and D) Mammalian two-hybrid analysis for M mutants and AIP1-WT. SeV M mutants and AIP1-WT were subcloned into pVP16 (AD) and pM (BD) vectors. 293T cells were co-transfected with the indicated AD and BD plasmids together with a pG5SEAP reporter plasmid. At 48 hr p.t., SEAP activity in the culture medium was determined using a fluorometer. Bars represent an average of three independent experiments. Expressions of Alix/AIP1 and M mutants were confirmed by Western blotting using anti-HA mAb for Alix/AIP1 and anti-SeV pAb for M mutants.

Fig. 4. Mammalian two-hybrid analysis for M-WT and a series of deletion mutants of Alix/AIP1. (A) Schematic representation of AIP1-WT and the Alix/AIP1 deletion mutants used in this study. Bro-like domain, Coiled-Coil domain, and Pro-rich domain reported by Katoh *et al*. (26) are highlighted in gray. (B and C) 293T cells were co-transfected with BD-fused M-WT and the indicated AD plasmids together with a SEAP reporter plasmid. Expressions of M protein and Alix/AIP1

mutants were confirmed by Western blotting as in Fig. 3. SEAP activity in the culture medium was determined using a fluorometer at 48 hr p.t. Bars represent an average of three independent experiments.

Fig. 5. Effect of overexpression of Alix/AIP1 mutants on budding of SeV M-VLPs. (A) 293T cells were co-transfected with M-WT and the indicated Alix/AIP1 mutants. At 24 hr p.t., cells were radio-labeled for another 24 hr. Cell lysates and VLPs were immunoprecipitated with anti-SeV pAb for M protein and anti-HA mAb for Alix/AIP1 mutants. (B) M proteins present in VLPs and cell lysates were quantitated. The values of M proteins in VLPs were normalized by those in cell lysates, and the levels of M protein in VLPs from cells transfected with an empty vector, (-), was set to 1. Bars represent an average of three independent experiments.

Fig. 6. Effect of Alix/AIP1 depletion on budding of SeV M-VLP. (A) 293T cells were transfected with Alix/AIP1-specific (#2147) or non-specific (NS) siRNA plasmids. At 24 hr p.t., cells were further co-transfected with M-WT and siRNA plasmids, and radio-labeled. Immunoprecipitation of M protein from VLPs (lanes 1 and 2) and cell lysates (lanes 3 and 4) are indicated. M proteins in VLPs and cell lysates were quantitated. The values of M proteins in VLPs were normalized by those in cell lysates. The level of M protein in VLPs from NS siRNA plasmid-transfected cells was set to 1. Bars represent an average of three independent experiments. (B) Western blot demonstrating that Alix/AIP1 from the transfected plasmid is inhibited following transfection of AIP1#2147, but is not

inhibited following transfection of NS-siRNA. (C) Coomassie blue stain of total protein extract from NS-siRNA transfected cells and AIP1#2147-transfected cells.

Fig. 7. Mammalian two-hybrid analysis for C-WT and a series of deletion mutants of Alix/AIP1. 293T cells were co-transfected with BD-fused C-WT and the indicated AD plasmids together with a SEAP reporter plasmid. (A) Expressions of C protein and Alix/AIP1 mutants were confirmed by Western blotting using anti-BD mAb for C-WT and anti-HA mAb for Alix/AIP1 mutants. (B) SEAP activity in the culture medium was determined using a fluorometer at 48 hr p.t. Bars represent an average of three independent experiments.

Fig. 8. Budding assay of M-WT and M-A4 in the presence or absence of other viral proteins. 293T cells were co-transfected with the indicated plasmids. At 48 hr p.t., VLPs (A) in the culture medium and cell lysates (B) were harvested, and analyzed by SDS-PAGE followed by Western blotting using anti-SeV and -C pAbs. (C) M proteins in VLPs and cell lysates were quantitated by densitometry with ImageJ software. The values of M protein in VLPs were normalized by those in cell lysates. The level of M-WT from cells not transfected with any additional viral proteins, (-), was set to 1. Bars represent an average of three independent experiments.

Fig. 1. Irie et al.

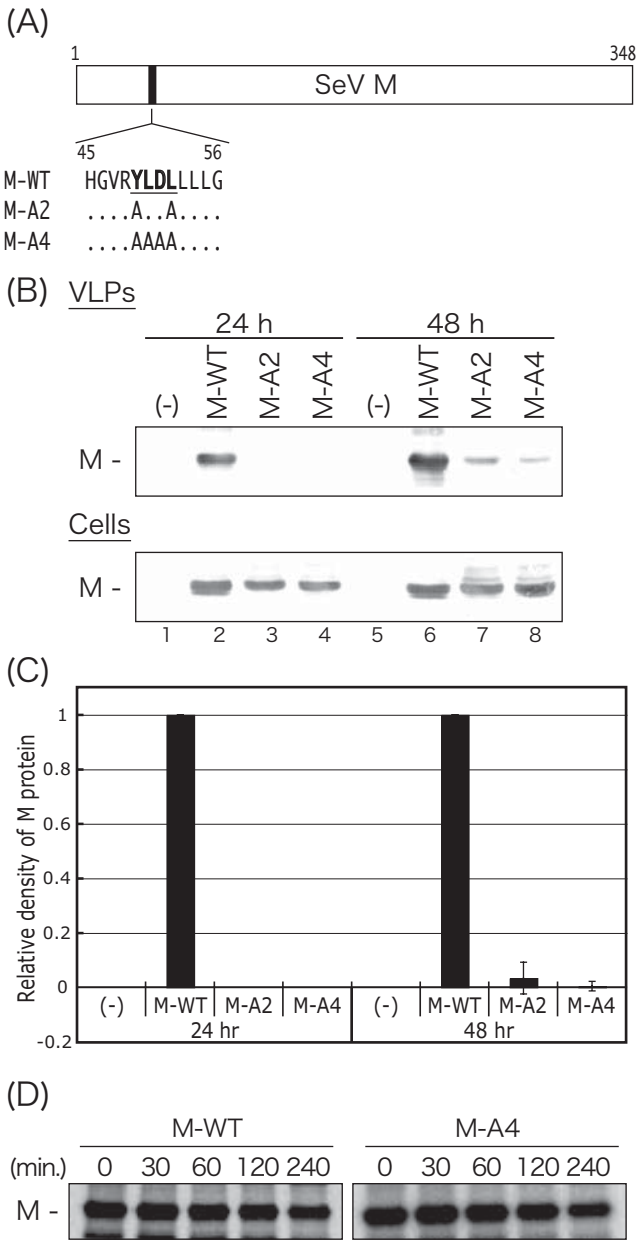

Fig. 2. Irie et al.

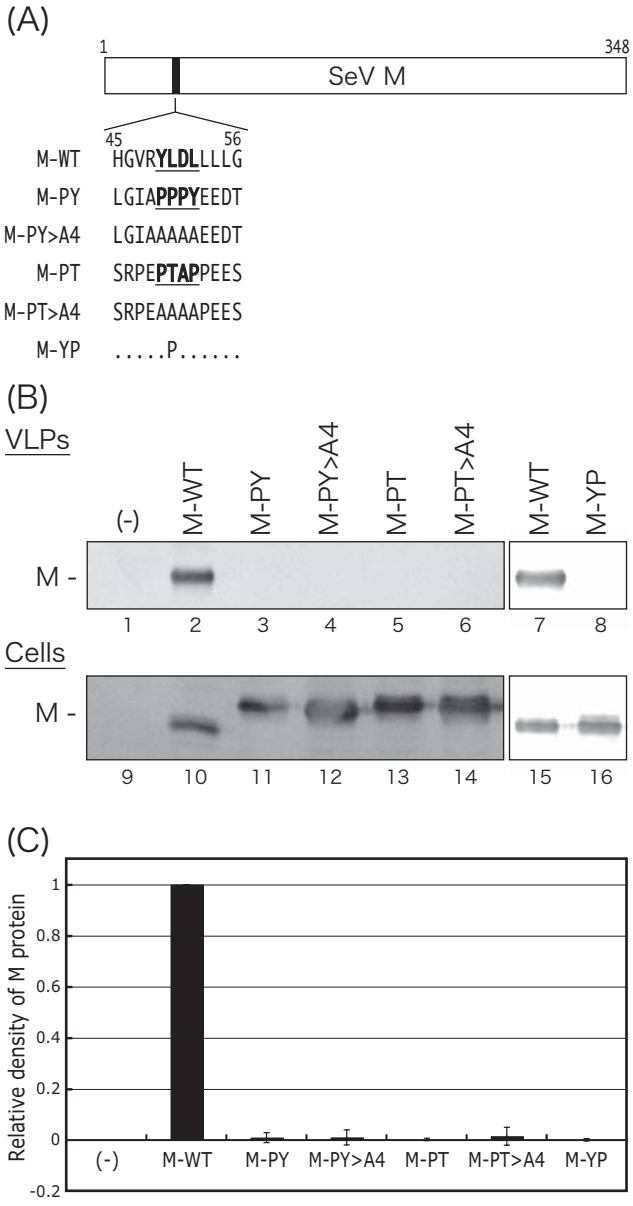

Fig. 3. Irie et al.

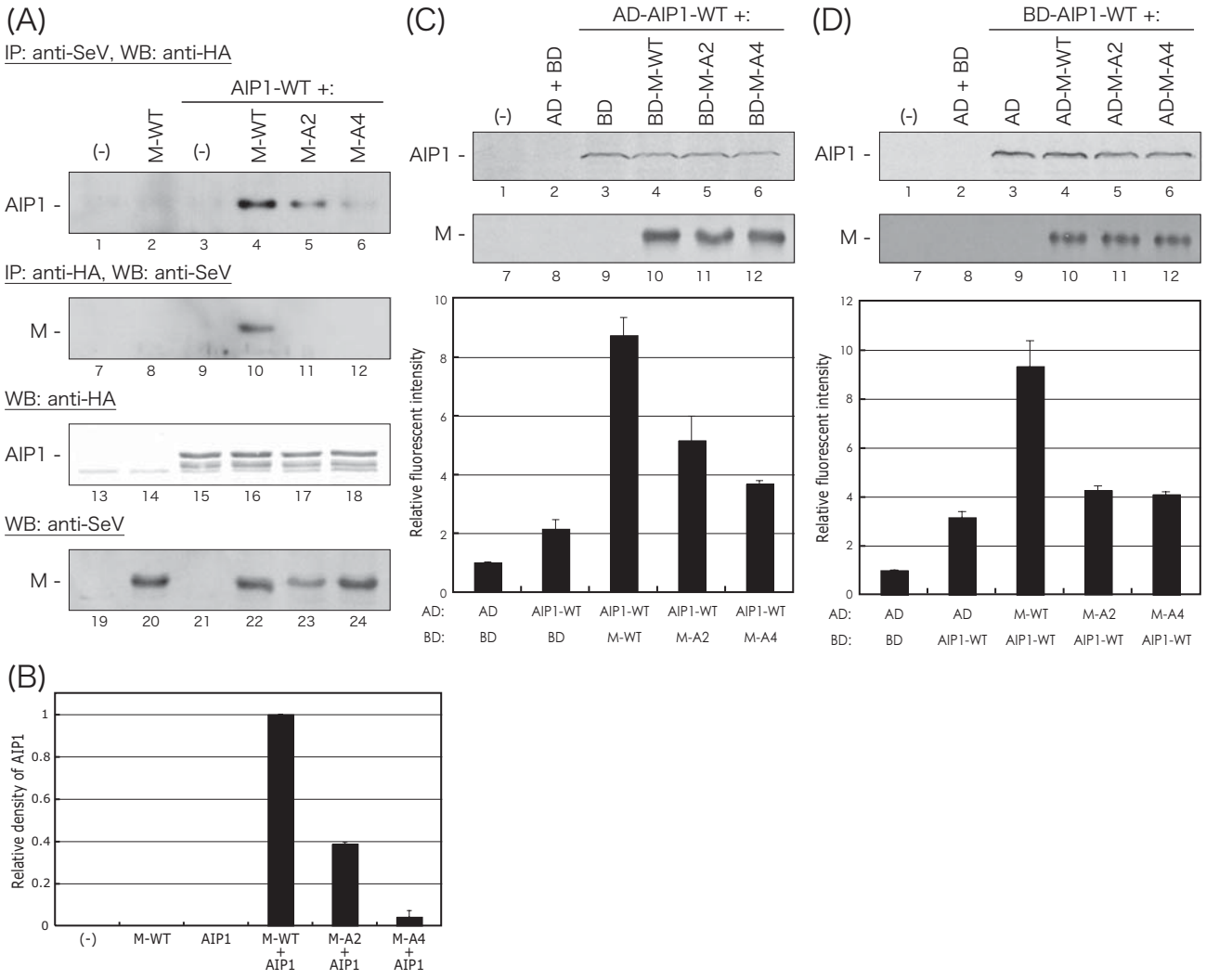

Fig. 4. Irie et al.

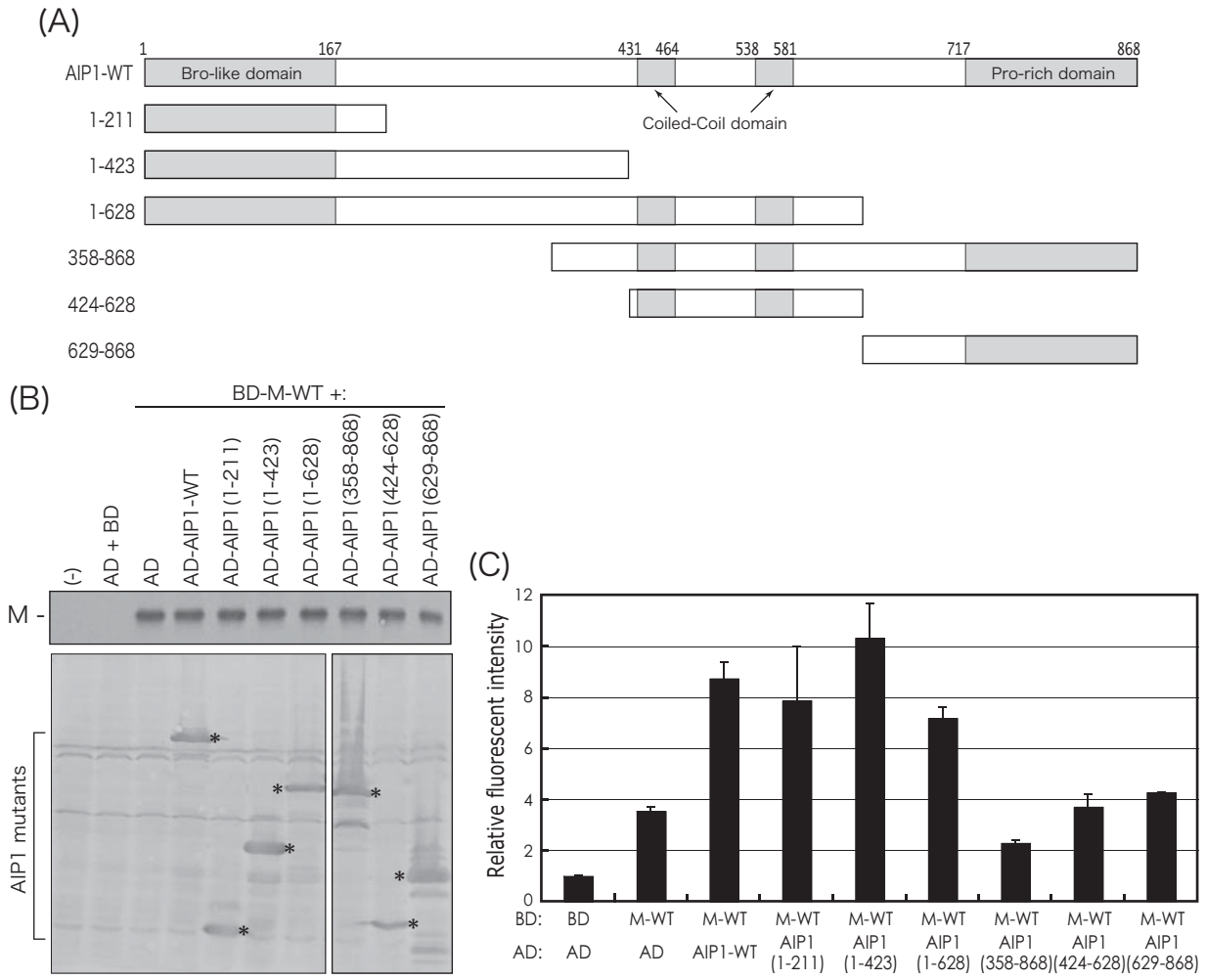

Fig. 5. Irie et al.

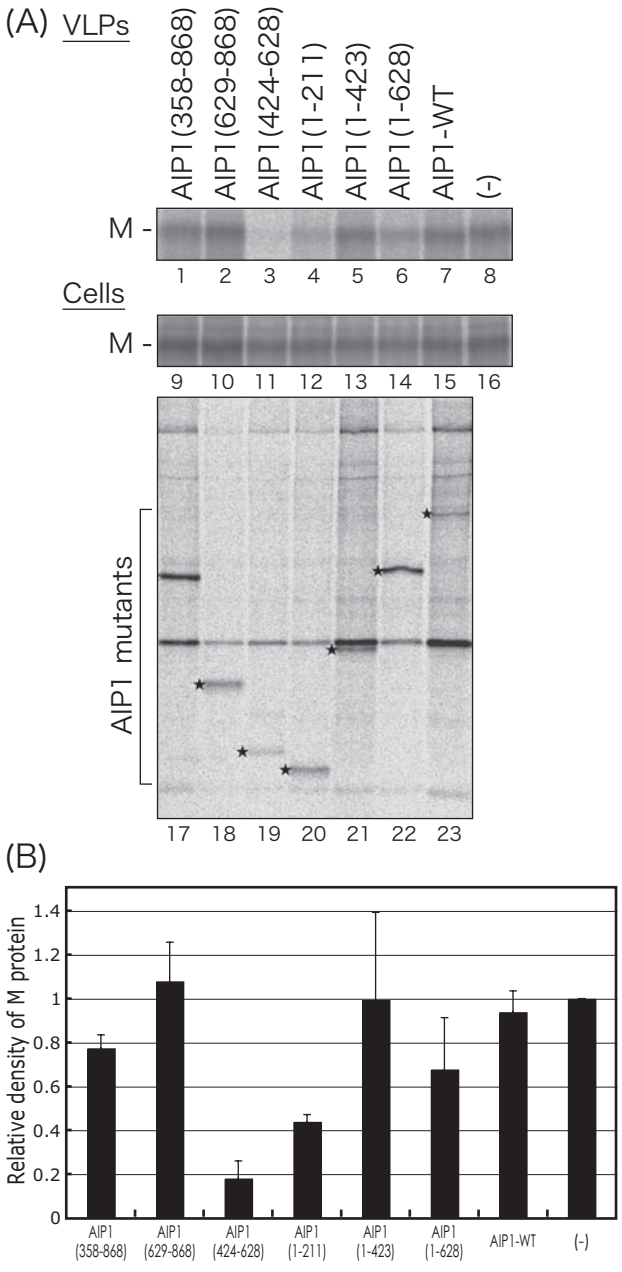

Fig. 6. Irie et al.

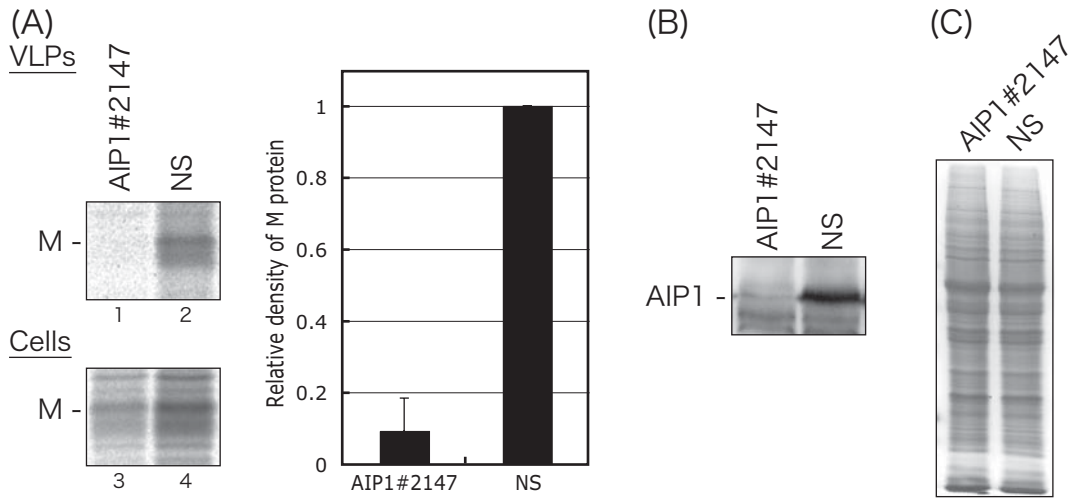

Fig. 7. Irie et al.

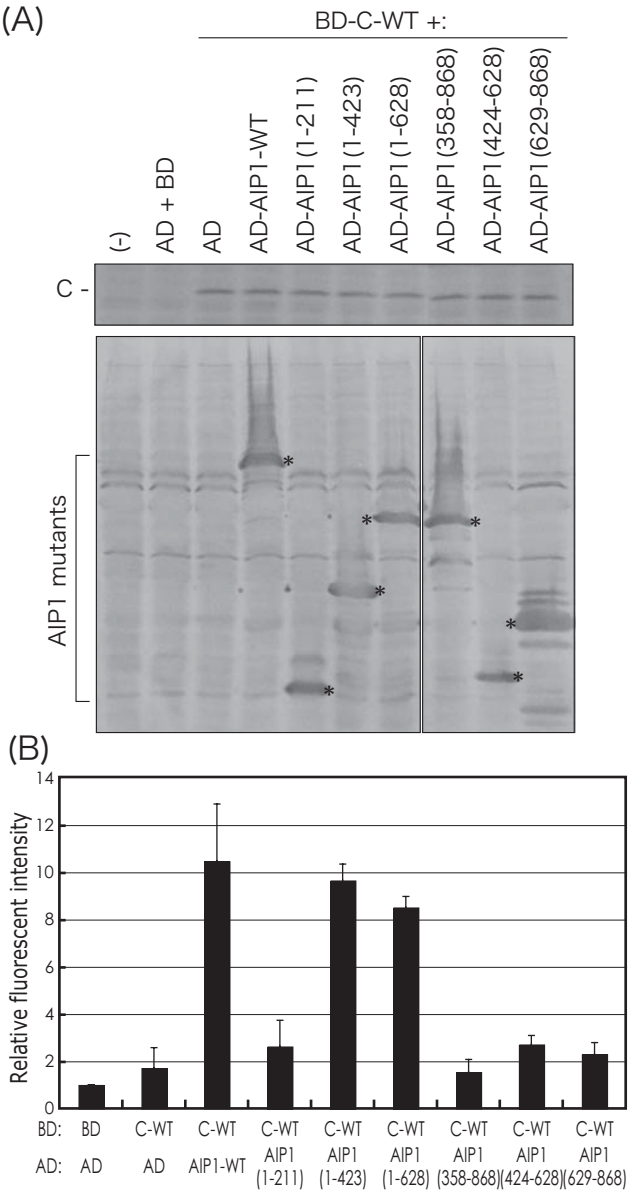

Fig. 8. Irie et al.